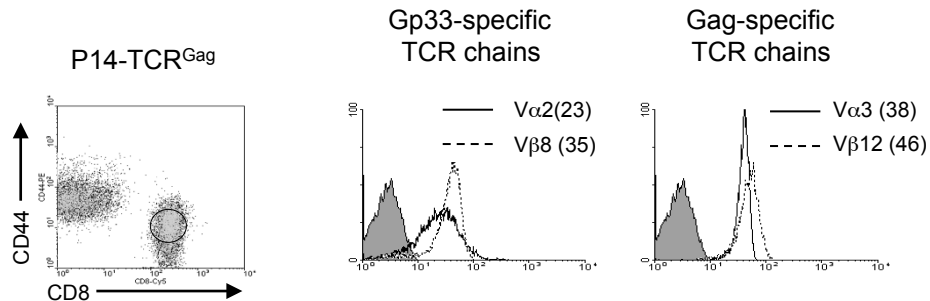
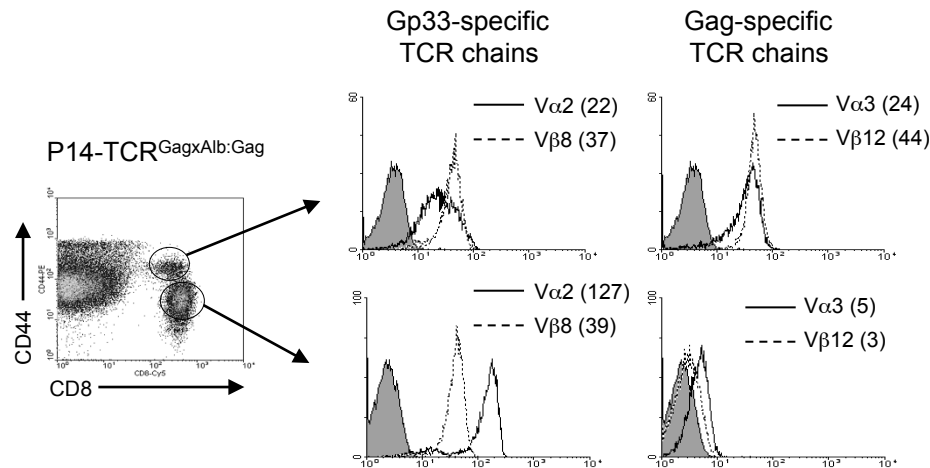


Supplementary Fig. 1

A

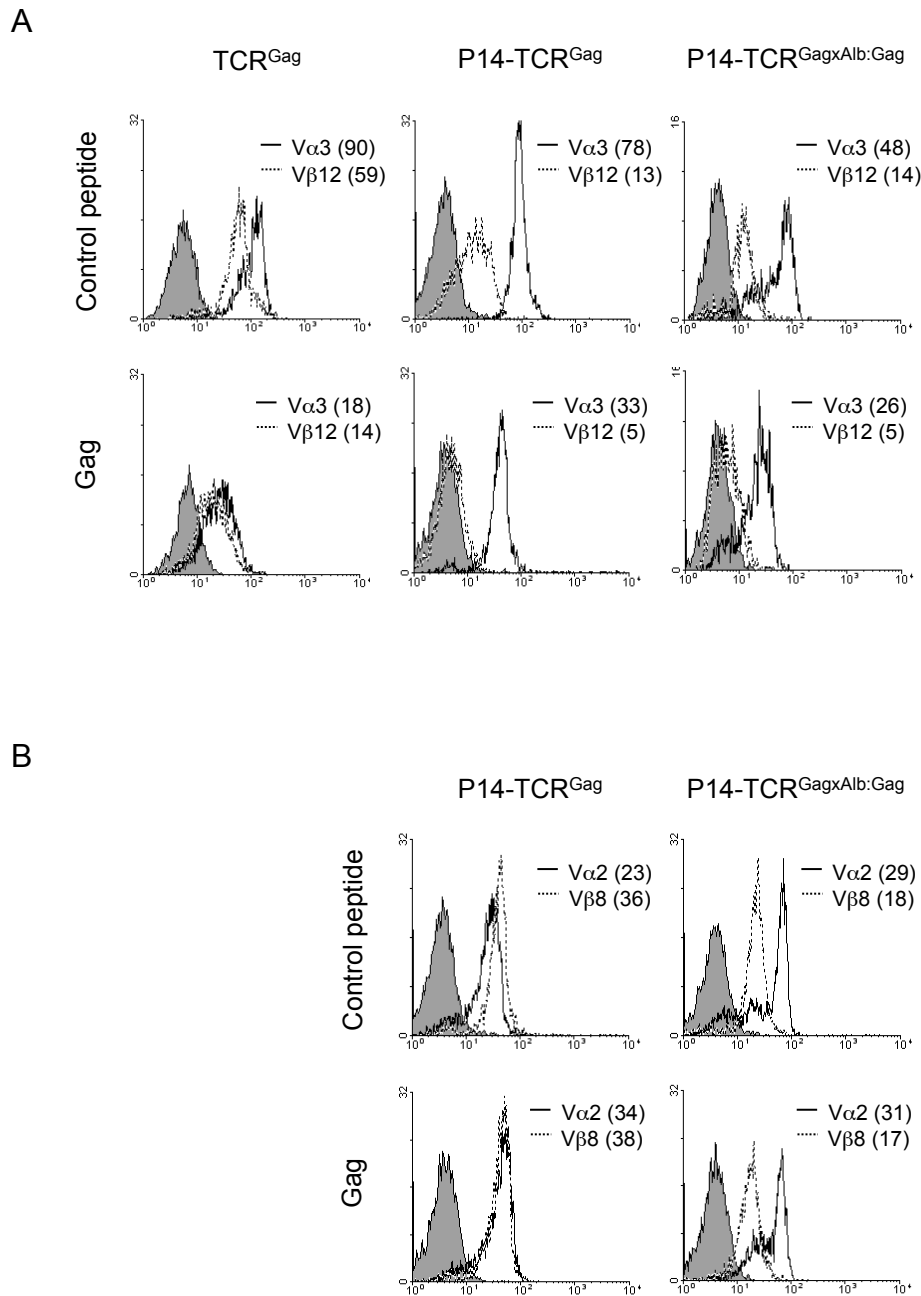


B



Supplementary figure 1. Strategy for sorting naive and tolerant CD8⁺ dual-TCR T cells based on CD44 expression profiles. (A) Naive P14-TCR^{Gag} and (B) tolerant P14-TCR^{GagxAlb:Gag} CD8⁺ splenocytes were analyzed by gating on distinct CD44^{low} and CD44^{hi} populations, respectively. Surface expression of Vα3/Vβ12 TCR^{Gag} chains (histograms on right) and Vα2/Vβ8 P14 chains (histograms on left) was analyzed by staining with specific TCR chain antibodies (lines) and compared to isotype control staining (grey). The MFI of each peak is indicated in parentheses.

Supplementary Fig. 2

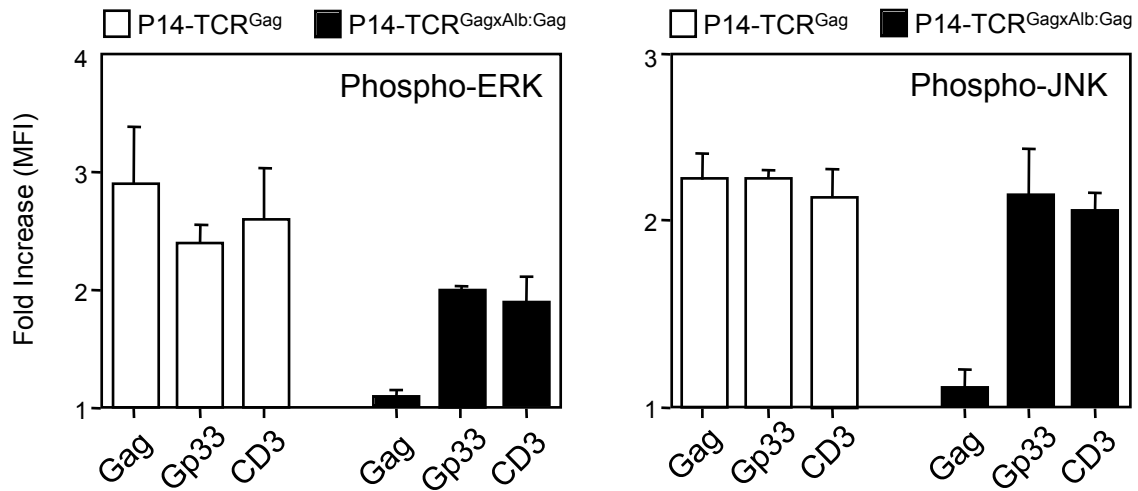


Supplementary figure 2. TCR down-modulation following *in vitro* Gag-peptide stimulation. Naive P14-TCR^{Gag} and tolerant P14-TCR^{GagxAlb:Gag} splenocytes were FACS sorted based on CD44 and CD8 expression profiles. Surface expression of (A) Vα3/Vβ12 and (B) Vα2/Vβ8 was analyzed by staining with specific TCR chain antibodies (lines) and compared to isotype control staining (grey) on single-receptor TCR^{Gag}, and P14-TCR^{Gag} and P14-TCR^{GagxAlb:Gag} dual-TCR T cells following 20 hour stimulation with 1 μg/ml control peptide or specific Gag peptide. The MFI of each peak is indicated in parentheses.

Supplementary Fig. 3

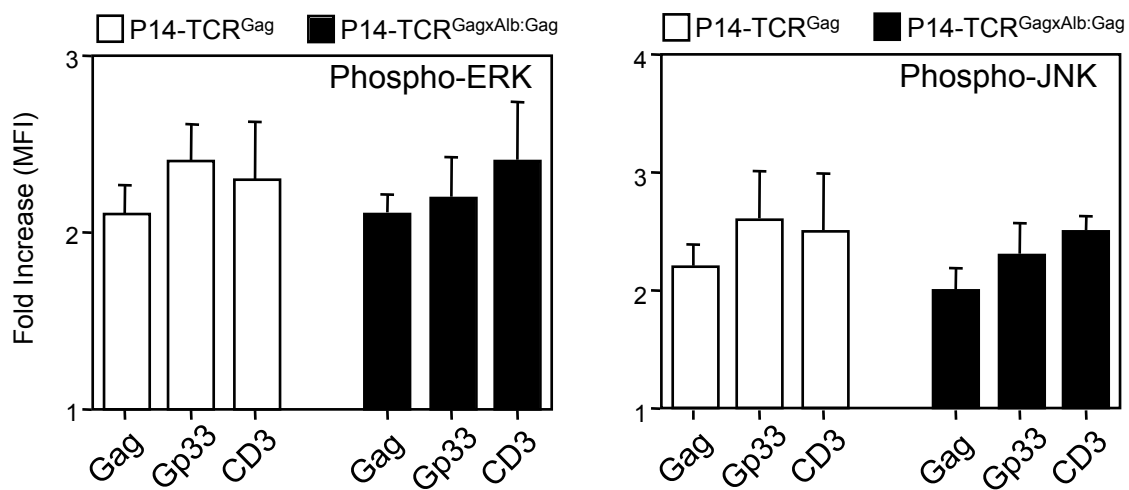
A

Resting cells



B

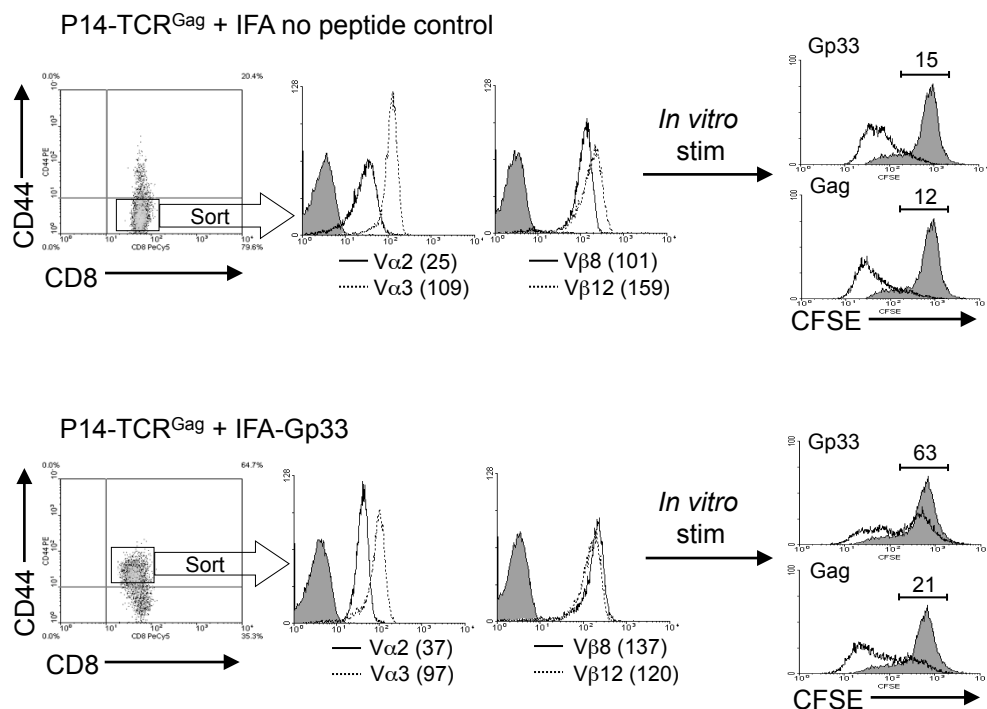
Expanded cells: Day 7 post-LCMV



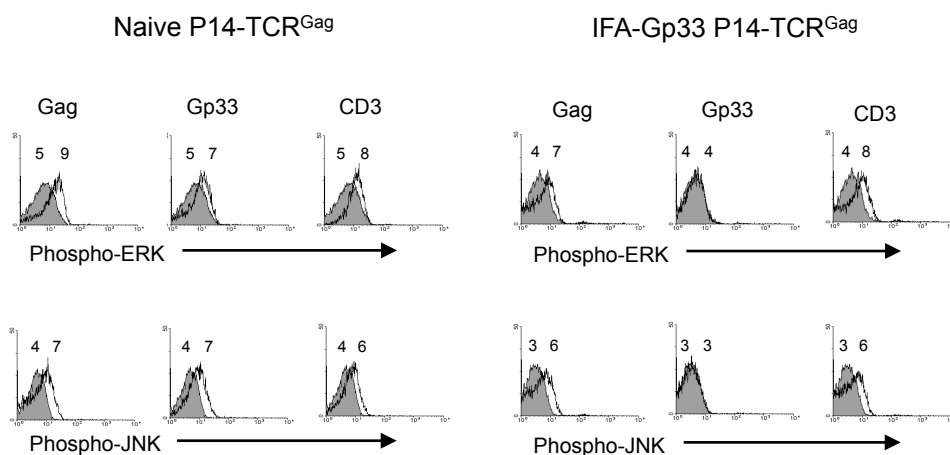
Supplementary figure 3. Statistical analysis of ERK and JNK phosphorylation following TCR triggering of resting or expanded dual-TCR T cells. Graphs represent fold-increase of ERK and JNK phosphorylation in P14-TCR^{Gag} (open bars) and P14-TCR^{GagxAlb:Gag} (closed bars) in response to 30 min *in vitro* stimulation with Gag or Gp33 peptide or anti-CD3, relative to control Env peptide, as described in Figures 3 and 4, of (A) resting or (B) T cells expanded *in vivo* for 7 days in response to LCMV. Data is presented as mean fluorescence intensity (MFI), and is pooled from 3 separate experiments (error bars represent SEM).

Supplementary Fig. 4

A



B

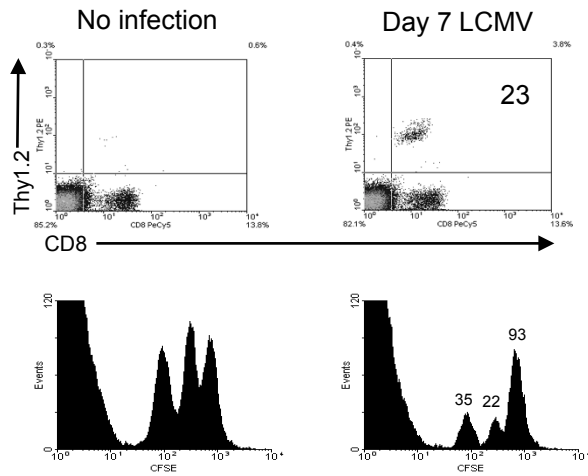


Supplementary figure 4. Alternative tolerization of dual-TCR T cells through the P14 TCR. Transgenic P14-TCR^{Gag} mice received incomplete Freund's adjuvant (IFA) alone or IFA plus Gp33-peptide by 3 repeated i.p. injections at 3 day intervals. Ten days after the last injection, splenocytes were removed and (A) expression of Vα2, Vα3, Vβ8 and Vβ12 (lines) assessed on CD44^{low} and CD44^{hi} CD8⁺ T cells. The isotype control Ab is in filled grey and MFI values are in parentheses. CD44^{low} naive and CD44^{hi} tolerized CD8⁺ T cells were purified by FACS sorting, labeled with CFSE and stimulated with control peptide (grey) or with Gag or Gp33 (lines) peptide-pulsed congenic APC, and CFSE dilution in Thy1.2⁺ cells assessed by flow cytometry. The percent of antigen stimulated cells (black lines) that had not diluted CFSE relative to cells stimulated with control peptide (grey) is indicated above the region. (B) FACS sorted CD44^{low} naive and CD44^{hi} IFA-Gp33 tolerized CD8⁺ T cells (Thy1.2) were combined 1:10 with APC from congenic mice, and stimulated with either control peptide (grey filled), Gag or Gp33-peptide (black lines) or anti-CD3 (black lines) *in vitro*. Phosphorylation of ERK and JNK in cells gated for Thy1.2 and CD8 expression (left) was assessed after 30 min by intracellular staining with phospho-specific antibodies. Numbers within the histograms represent the MFI for each peak.

Supplementary Fig. 5

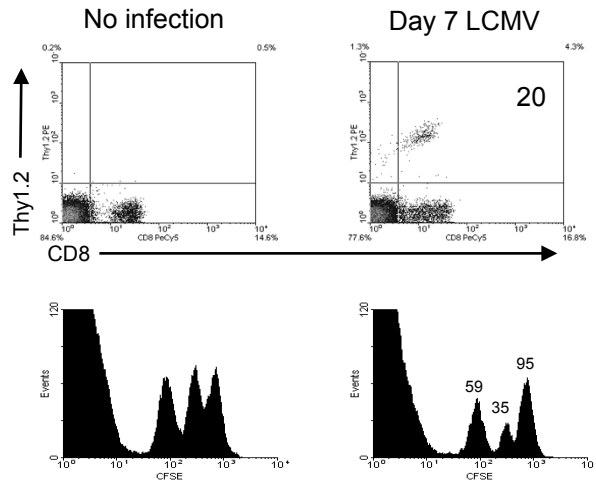
A

Thy1.1 recipients + P14-TCR^{Gag} donor T cells



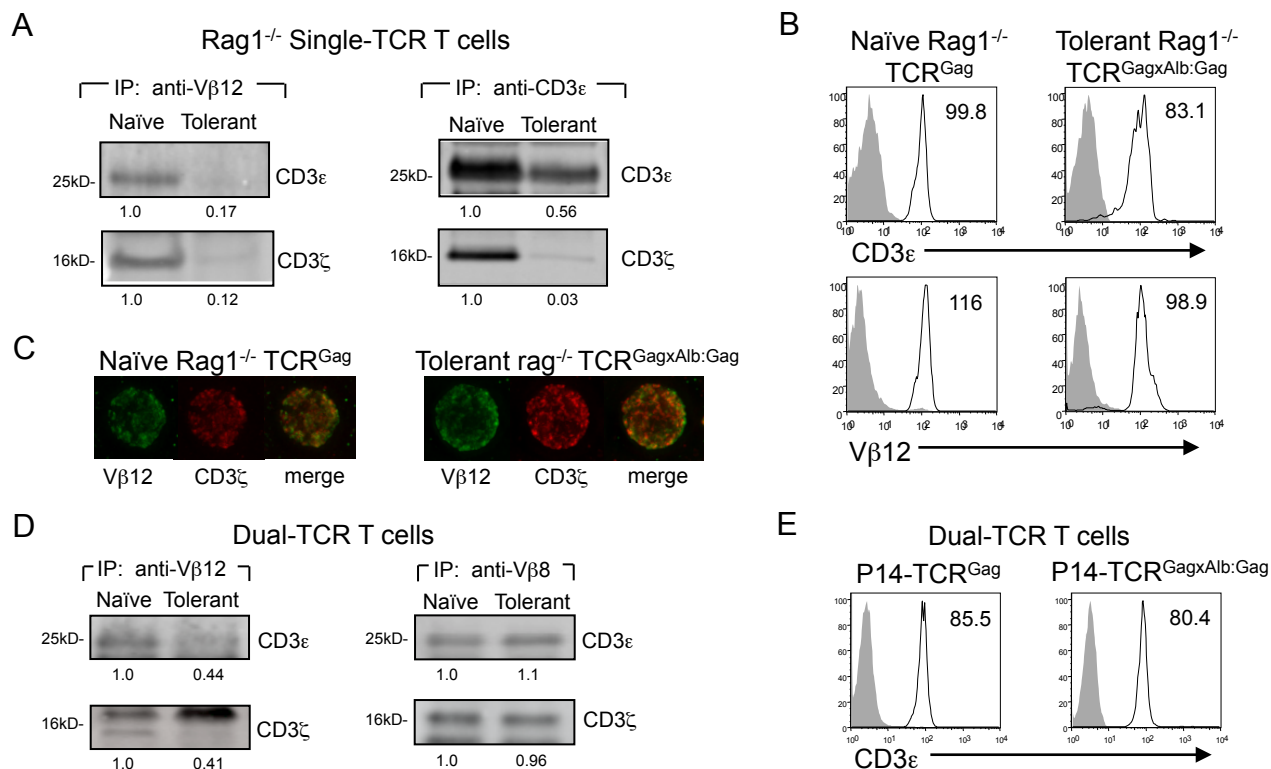
B

Alb:Gag^{Thy1.1} recipients + P14-TCR^{GagxAlb:Gag} T cells



Supplementary figure 5. *In vivo* lytic activity of dual-TCR T cells following expansion in response to LCMV infection. Transgenic naive P14-TCR^{Gag} and tolerant P14-TCR^{GagxAlb:Gag} splenocytes were FACS sorted based on CD44 and CD8 expression, and 1×10^5 purified T cells transferred into the indicated (A) Thy1.1 or (B) Alb:Gag^{Thy1.1} recipients, and either left uninfected or infected with LCMV. At day 7 post-infection, PBL from all recipients were analyzed for the frequency of CD8⁺ Thy1.2⁺ cells, and numbers in the upper-right quadrants represent percent of total CD8⁺ cells. On day 7, recipient mice were infused with differently labeled peptide-pulsed target cells. Briefly, splenocytes from a Thy1.1⁺ mouse were pulsed with 0.1 or 10 $\mu\text{g}/\text{ml}$ Gag-peptide or with control peptide and then labeled with 2, 6 or 18 $\mu\text{g}/\text{ml}$ CFSE, respectively. 20 hours after target cell infusion, recipient splenocytes were analyzed for target cell frequency. Numbers above each CFSE peak represents the percent of each target cell population relative to the corresponding population in non-infected mice.

Supplementary Fig. 6



Supplementary figure 6. Selective instability of the tolerant TCR complex. To examine pure naïve and tolerant TCR complexes, we isolated complexes initially from Rag1^{-/-} naïve TCR^{Gag} and tolerant TCR^{GagxAlb:Gag} single-TCR T cells (expressing only transgenic naïve or tolerant TCR complexes; see Fig. 1). Briefly, (A) Rag1^{-/-} naïve and tolerant CD8⁺ T cells were lysed in 6 mM CHAPS buffer and immuno-precipitated with anti-Vβ12 or anti-CD3ε, and associated proteins that co-precipitated separated by SDS-PAGE and blotted to PVDF membranes. Membranes were stained with anti-CD3ε or anti-CD3ζ, followed by fluorescently-conjugated secondary antibodies, detected on a Licor Odyssey system, and analyzed using Image J software. Substantially less CD3ε and CD3ζ co-precipitated with anti-Vβ12 in tolerant compared to naïve cells, and CD3ζ also failed to co-precipitate with CD3ε selectively in tolerant TCR complexes- the values below blots represent the densitometric ratio of each band pair, with the ratio in naïve cells set at 1.0. Additionally, less total CD3ε precipitated from tolerant cells, which may in part reflect reduced surface expression (see B) or possible post-translational modifications that mitigate antibody binding. (B) Rag1^{-/-} transgenic T cells were analyzed to determine the relationship of surface CD3ε (line) to Vβ12 (line) in naïve and tolerant cells (isotype control antibody staining in grey). The MFI for each peak is indicated within the histograms, with the slight reduction in CD3ε detected in tolerant cells proportional to the slight reduction in Vβ12, indicating that the failure to detect CD3ε in tolerant complexes precipitated with anti-Vβ12 in (A) is not explained by loss of surface expression. (C) Confocal microscopy was used to evaluate total expression and distribution of Vβ12 (green) and CD3ζ (red) on permeabilized Rag1^{-/-} naïve and tolerant CD8⁺ T cells. Expression appeared nearly equivalent, suggesting the lack of CD3ζ to co-precipitate with tolerant TCR complexes was not due to lack of cellular CD3ζ. The results suggest compromised integrity of the TCR complex in tolerant T cells, as reflected by failure to co-precipitate essential TCR signaling components. To examine if this defect reflected specific modification of the TCR complexes that had engaged a tolerogen or a global change to tolerant cells, (D) transgenic naïve CD44^{low} P14-TCR^{Gag} and tolerant CD44^{high} P14-TCR^{GagxAlb:Gag} dual-TCR CD8⁺ T cells were FACS sorted, lysed in 6 mM CHAPS buffer and immunoprecipitated with anti-Vβ12 or anti-Vβ8 antibody, and the co-precipitated proteins separated by SDS-PAGE and blotted to PDVF membranes. Blots were stained with anti-CD3ε and anti-CD3ζ. Analysis of the proteins present in each complex relative to naïve cells again revealed reduced CD3ε and CD3ζ in the tolerant complexes. (E) Naïve CD44^{low} and tolerant CD44^{high} dual-TCR T cells were stained for surface CD3ε (line), with isotype control antibody staining in grey. Nearly equivalent CD3ε expression was detected in naïve and tolerant dual-TCR T cells, which similarly express nearly equivalent amounts of Vβ12 and Vβ8 (Fig. Suppl. 1). The slightly more CD3ε and CD3ζ co-precipitating with anti-Vβ12 in tolerant dual-TCR cells compared to single-TCR cells on a Rag1^{-/-} background likely reflects in part some mis-matched TCR chain pairing in the Rag1⁺ dual-TCR cells so that a small number of Vβ12 - containing complexes may not be part of a Gag-specific and thus tolerant TCR complex. These results therefore suggest that the tolerant TCR complexes in dual-TCR T cells are selectively modified and, similar to tolerant single-TCR cells, exhibit compromised integrity of associations between critical signaling components.